ISSN No:-2456-2165 https://doi.org/10.38124/ijisrt/26aug534

Helical Cutter Geometry and Process Conditions in Peripheral Milling: A Mechanistic Framework for Surface Texture Formation

Ali Serhat Ersoyoğlu[1]

[1]Konya Technical University, Konya, Türkiye

Corresponding Author: Ali Serhat Ersoyoğlu*

Publication Date: 2026/08/21

Abstract: Surface texture in peripheral milling emerges from the combined action of cutter kinematics, engagement, force generation, structural response, tool condition, and geometric error. The cutter helix is of particular interest because it distributes an individual cutting edge along the axial direction and consequently introduces a phase difference between axial sections of that edge. This review re-examines published evidence through that geometric–mechanical connection. Rather than reporting new measurements or fitting a universal roughness equation, the paper organizes analytical, numerical, and experimental findings into a causal sequence: helix geometry affects axial engagement and chip-load phase; the resulting load distribution interacts with machine–tool dynamics; the actual tool trajectory then determines the surface texture. Feed per tooth, cutting speed, axial and radial engagement, runout, vibration, and tool wear are treated as interacting variables rather than isolated predictors. A literature-derived functional framework is formulated to show where these variables enter the surface-generation process and which relationships still require experimental calibration. The review therefore serves as a mechanistic synthesis and as a design basis for a future controlled study, not as a validated predictive model.

Keywords: *Peripheral Milling; Helical Cutter; Helix Angle; Surface Texture; Surface Roughness; Feed Per Tooth; Cutting Dynamics; Runout; Mechanistic Framework.*

How to Cite: Ali Serhat Ersoyoğlu (2026) Helical Cutter Geometry and Process Conditions in Peripheral Milling: A Mechanistic Framework for Surface Texture Formation. *International Journal of Innovative Science and Research Technology*, 11(8), 1236-1245. https://doi.org/10.38124/ijisrt/26aug534

I. INTRODUCTION

The discussion is deliberately arranged as a causal chain. Basic milling variables are defined first, followed by the geometry of a helical edge. The next stages consider chip thickness and force, dynamic response, surface generation, and the individual roles of feed, speed, and engagement. The final part compares the evidence, identifies unresolved questions, and specifies how the proposed framework could be tested experimentally.

In peripheral milling, the workpiece surface is formed by repeated edge passages while the cutter and workpiece undergo elastic and dynamic motion. Consequently, the surface cannot be attributed to one machine setting. Cutter geometry, radial and axial engagement, feed, cutting speed, force-induced deflection, vibration, runout, and edge condition can all modify the trajectory traced by the cutting edge.

The literature on roughness prediction has repeatedly shown that process variables and machine-state information are relevant. Zhang et al. [1] used Taguchi-based optimization to examine milling variables, Ozcelik and Bayramoglu [2] incorporated process and tool-operating variables into statistical roughness modelling, and Brezocnik et al. [3] demonstrated the value of including vibration information. These studies establish the importance of process conditions but do not, by themselves, explain how helical-edge geometry changes the mechanism.

Helical geometry supplies that missing geometric link. The side-milling model of Buj-Corral et al. [4] connects feed, eccentricity, and helix angle with generated topography, while Wan et al. [5] examined the influence of helix on peak cutting force. Ozturk et al. [6] and Kao et al. [7] likewise showed that helix-dependent geometry must be considered when estimating cutting-force coefficients.

The central question of this review is therefore not whether helix angle matters, but where its influence enters the surface-generation chain and how that influence interacts with process variables. The analysis is intended to separate

ISSN No:-2456-2165 https://doi.org/10.38124/ijisrt/26aug534

direct geometric effects from force-, dynamics-, wear-, and runout-related effects.

Novelty and contribution. The contribution is a mechanism-oriented synthesis rather than a new empirical correlation. Studies addressing surface topography, cutting force, variable-helix stability, and roughness prediction are brought into one causal scheme. Established relationships are distinguished from proposed links that need calibration. This distinction is important because it prevents a literature review from being presented as if it were an experimentally validated model.

II. REVIEW METHODOLOGY

A structured literature-screening procedure was used to assemble studies relevant to helical cutter geometry and surface formation in peripheral milling. The scope was intentionally not restricted to one alloy or one cutter architecture because the intended outcome is a transferable mechanistic map.

Search combinations included helix angle, variable helix, peripheral milling, side milling, cutting force, surface roughness, surface topography, milling stability, and tool runout. Publisher records and scholarly indexing services were consulted, and a study was retained only when its bibliographic identity could be checked sufficiently to associate the cited work with a stable publication record and DOI information where available.

The evidence was retained when a study contributed to at least one of four questions: how helix geometry affects force; how helix geometry affects surface generation; how helix or pitch variation affects regenerative dynamics; or how conventional milling variables enter roughness prediction. Work outside these topics, or records lacking enough bibliographic information for reliable identification, was not used in the mechanistic synthesis.

The selected studies were then read as four connected evidence streams: geometric surface generation, mechanistic force modelling, dynamic and stability analysis, and empirical/statistical roughness prediction. The 2025 publications [34], [35] were considered separately as recent evidence because they extend the discussion toward gradient-helix force modelling and the coupled role of helix, cutting conditions, and wear.

➢ *Fundamentals of Peripheral Milling*

The variables required to interpret the subsequent equations and figures are defined in Fig. 1.

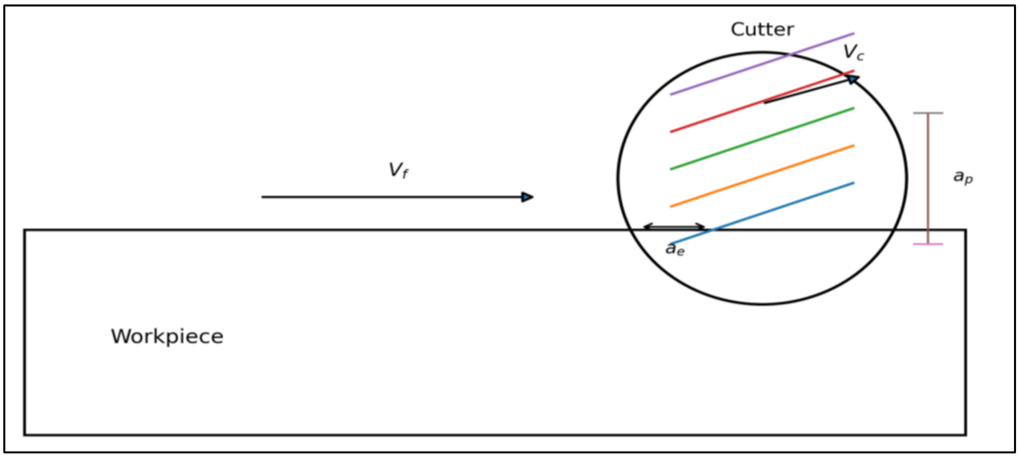

Fig 1 Schematic Representation of Peripheral Milling Showing Feed Velocity (V_f), Cutting Speed (V_c), Radial Depth of Cut (a_e), and Axial Depth of Cut (a_p).

A rotating cutter establishes the circumferential cutting motion, while the programmed feed produces the relative translation of the workpiece. For cutter diameter D and spindle speed n, the nominal cutting speed is

$$V_c = \pi D n / 1000 \tag{1}$$

Here, V_c denotes cutting speed in m/min, D is cutter diameter in mm, and n is spindle speed in rev/min. The corresponding feed relation is

$$V_f = f_z z n \tag{2}$$

Here, V_f is feed velocity in mm/min, f_z is feed per tooth in mm/tooth, and z is the number of teeth.

Thus, f_z = V_f/(zn). In geometric terms, f_z sets the nominal distance advanced by the workpiece between successive tooth engagements.

For a simplified constant-width engagement, the material-removal rate can be written as

$$MRR = a_p a_e V_f \tag{3}$$

In Eq. (3), MRR is material-removal rate, a_p is axial depth of cut in mm, and a_e is radial depth of cut in mm.

MRR is introduced only as a productivity measure; it is not treated as a direct roughness law.

ISSN No:-2456-2165 https://doi.org/10.38124/ijisrt/26aug534

➢ *Helix-Angle Geometry*

Figure 2 uses an unwrapped cylindrical representation so that the helix geometry can be read without perspective distortion. Here β is defined as the angle between the helical edge and the circumferential reference direction; p_a denotes axial pitch and p_c the corresponding circumferential advance.

The same general principle—that tool-axis orientation can alter engagement, force, surface generation, and stability—also appears in five-axis ball-end milling through lead and tilt effects [10].

Figure 2 defines the adopted angle convention, while Fig. 3 visualizes the resulting axial phase shift for several helix angles.

Because a helical edge advances circumferentially as it moves axially, different axial locations of the same tooth encounter the workpiece at different angular positions. That phase difference is the geometric feature used throughout the proposed framework.

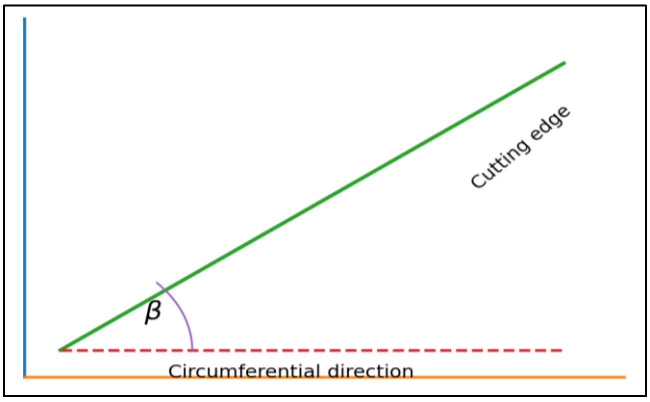

Fig 2 Unwrapped Cylindrical Representation of the Helical Cutting Edge, Showing the Helix Angle (β), Axial Pitch (p_a), and Circumferential Pitch (p_c).

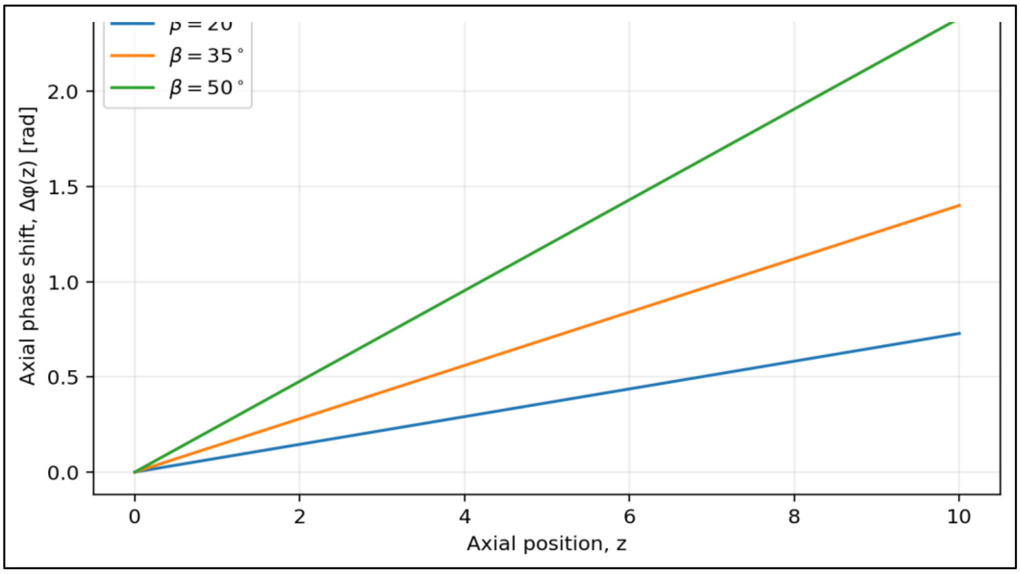

Fig 3 Axial Phase Shift of a Helical Cutting Edge as a Function of Helix Angle.

For an axial position z_a, a commonly used geometric representation of the phase shift is

$$\Delta\varphi(z\_a) = 2\, z\_a \tan(\beta) / D \quad (4)$$

In Eq. (4), Δφ is the phase difference in radians, z_a is axial position in mm, β is helix angle, and D is cutter diameter in mm.

The sign of Δφ depends on the selected coordinate convention. The magnitude, however, increases with helix angle and axial separation, which is the feature relevant to the subsequent chip-load and force discussion.

Helix-angle convention. Throughout the manuscript, β is measured on the developed cutter surface from the circumferential reference direction to the helical edge. Changing the coordinate convention changes the sign convention, not the physical conclusion that larger helix produces a larger axial phase difference.

This distributed phase is the point at which cutter geometry enters both surface generation and force redistribution. It is therefore more informative for the present purpose than treating helix angle as an isolated catalogue parameter.

➢ *Chip Thickness and Cutting-Force Mechanism*

Figure 4 shows the phase displacement of the instantaneous chip-load signal produced by different helix angles. Figure 5 then illustrates, schematically, how the same geometric change can redistribute force components.

For a simplified tooth-position description, instantaneous chip thickness can be represented as

$$h(\varphi, z\_a) \approx f\_z \sin[\varphi + \Delta\varphi(z\_a)] \quad (5)$$

ISSN No:-2456-2165 https://doi.org/10.38124/ijisrt/26aug534

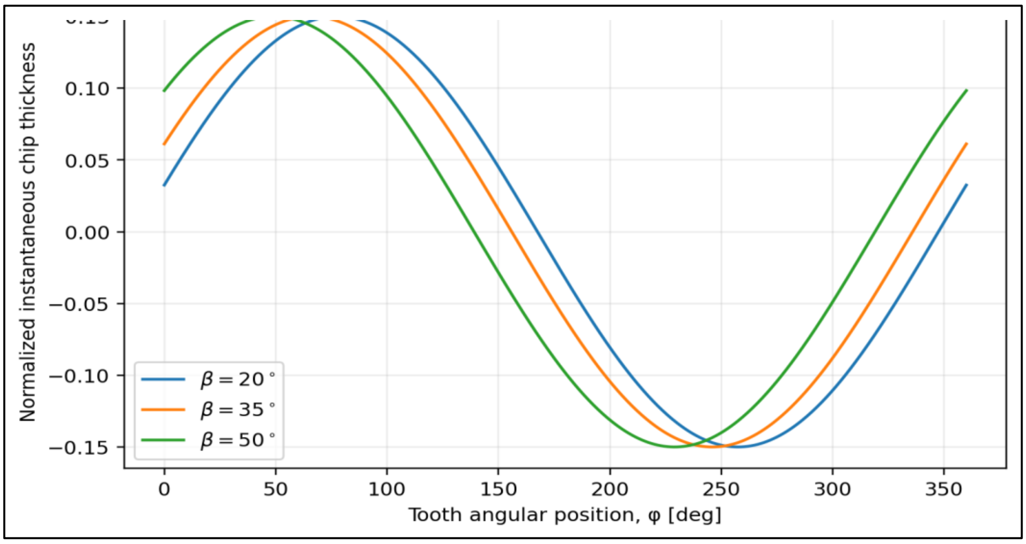

Fig 4 Schematic Effect of Helix Angle on Instantaneous Chip-Thickness Phase.

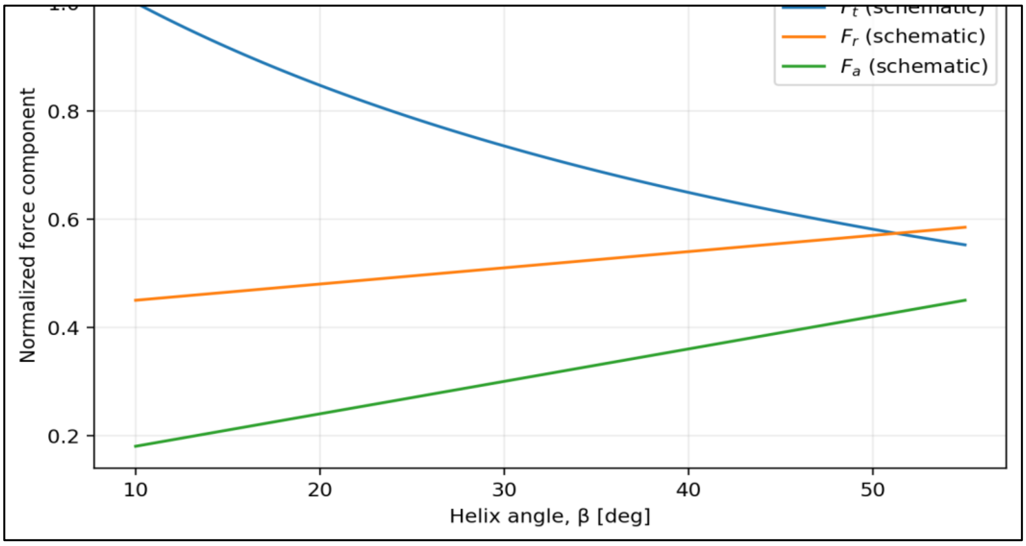

Fig 5 Conceptual Influence of Helix Angle on Cutting-Force Distribution.

In Eq. (5), h is instantaneous uncut chip thickness in mm; φ is tooth angular position in rad; z_a is axial position in mm; f_z is feed per tooth in mm/tooth; and Δφ is the helix-induced phase shift in rad.

Substitution of Eq. (4) gives

$$h(\varphi, z\_a) \approx f\_z \sin[\varphi + 2 z\_a \tan(\beta) / D] \quad (6)$$

Equation (6) uses the same definitions; β is helix angle and D is cutter diameter.

Equation (6) is intentionally limited to the phase mechanism. It is not a complete engagement model, because entry and exit limits, radial immersion, tooth indexing, and material-dependent cutting coefficients are not included in this simplified expression.

A differential tangential-force relation may then be written as

$$dF\_t = K\_t\, h(\varphi, z\_a)\, dz\_a \quad (7)$$

Here dF_t is the differential tangential force in N, K_t is the tangential cutting-force coefficient in N/mm², h is chip thickness in mm, and dz_a is an infinitesimal engaged axial length in mm.

The corresponding radial component can be written in the same form and integrated over the engaged axial interval. Published analyses report a measurable helix dependence in peak force and in the force coefficients used for tool modelling [5]–[7].

The force pathway is consistent with the classical mechanistic approach in which cutting coefficients are obtained from orthogonal-cutting information and then integrated over a helical edge [21]–[24]. Budak and Altintas [22] addressed coefficient identification from orthogonal cutting data, while Armarego and Deshpande [23] developed helical-tooth force formulations; Lamikiz et al. [24] considered specific cutting coefficients together with tool geometry.

ISSN No:-2456-2165 https://doi.org/10.38124/ijisrt/26aug534

For surface formation, the consequence is indirect but important: a change in the magnitude or phase of the cutting load can change elastic deflection and vibration. The edge then follows a trajectory different from the purely kinematic path used by an ideal geometric roughness calculation.

➢ *Dynamic Response and Milling Stability*

A simplified linear representation of the machining system is

$$M\,\ddot{x}(t) + C\,\dot{x}(t) + K\,x(t) = F(t) \qquad (8)$$

In Eq. (8), M, C, and K represent equivalent mass, damping, and stiffness terms of the machine–tool–workpiece system. The variable x(t) denotes dynamic relative displacement, and F(t) is the time-varying milling-force excitation.

The force term contains tooth-passing and regenerative components. The tooth-passing frequency is

$$f\_tp = z\,n\,/\,60 \qquad (9)$$

In Eq. (9), f_tp is tooth-passing frequency in Hz, z is tooth count, and n is spindle speed in rev/min.

Variable-pitch and variable-helix studies provide evidence that cutter geometry changes regenerative phase relationships. Sims et al. [8] treated variable pitch and helix in chatter prediction, Jin et al. [9] developed a frequency-domain solution, Yusoff and Sims [14] examined geometry for chatter mitigation, and Niu et al. [15] included runout in a multi-regenerative stability treatment.

This matters for roughness because chatter or other dynamic modulation changes the actual edge trajectory. Ideal feed marks therefore describe only the kinematic part of the generated texture.

➢ *Geometrical and Process-Induced Surface Roughness*

Figures 6 and 7 separate the causal pathway from the resulting geometric and dynamic surface components.

A measured roughness value can be viewed as the outcome of several mechanisms that coexist on the finished surface. Runout, displacement, force-induced motion, and process variability have all been incorporated into published surface-generation or reconstruction approaches [11]–[13], [32].

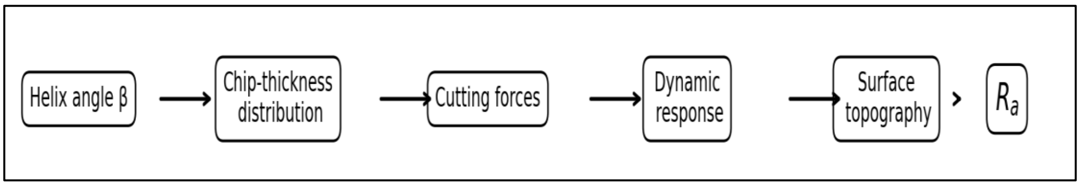

Fig 6 Mechanistic Pathway from Helix Angle to Surface Roughness.

$$R\_a \approx R\_a,g + R\_a,d + R\_a,w + R\_a,e \qquad (10)$$

Here R_a denotes the measured arithmetic average roughness. The subscripts g, d, w, and e refer respectively to geometric, dynamic, wear-related, and geometric-error contributions.

Equation (10) is a bookkeeping decomposition, not a claim that the four terms are physically independent or strictly additive. Its purpose is to expose mechanisms that may be hidden when only a single scalar roughness value is reported.

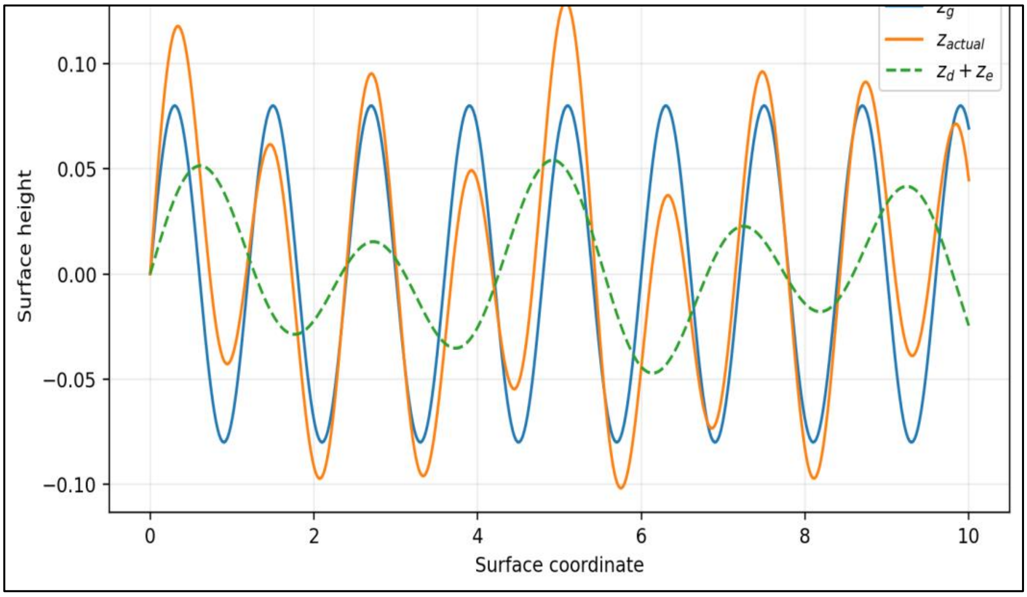

Fig 7 Geometrical and Dynamic Contributions to the Generated Surface Topography.

ISSN No:-2456-2165 https://doi.org/10.38124/ijisrt/26aug534

The geometric model of Buj-Corral et al. [4] demonstrates that feed, eccentricity, and helix angle can alter the height distribution of a side-milled surface. Other work has shown that runout can create spatial bands or heterogeneity in the topography [11], while measured force and displacement information can be used to reconstruct the generated surface [12], [13].

Runout-correction studies further indicate that geometric error and dynamic correction can change the effective cutting trajectory [16].

Dynamic displacement may be represented as x_d(t), so that

$$x\_actual(t) = x\_ideal(t) + x\_d(t) \qquad (11)$$

In Eq. (11), x_actual(t) is the actual relative tool/workpiece displacement, x_ideal(t) is the displacement predicted from ideal kinematics, and x_d(t) is the additional displacement associated with vibration and deformation.

Equation (11) provides the interface between a force/dynamic description and the surface that is ultimately measured.

➢ *Effect of Feed per Tooth*

Feed per tooth has a direct geometric role because it determines both the nominal chip thickness scale and the spacing between consecutive tooth paths. Experimental and predictive studies repeatedly identify feed among the important variables for milling roughness [1]–[3], [25]–[31]. A generic sensitivity form is

$$R\_a \propto f\_z\hat{}m \qquad (12)$$

In Eq. (12), R_a is arithmetic average roughness, f_z is feed per tooth, and m is an empirical exponent whose value depends on the process and material.

The cited prediction studies use different modelling strategies, but they converge on the need to account for process conditions. Examples include statistical optimization [1], statistical roughness modelling [2], genetic programming [3], grey-fuzzy modelling [26], intelligent-system comparisons [27], machine-vision and neural-network prediction [28], hybrid incremental modelling [29], and heterogeneous-data/Bayesian prediction [30]. The common point is not a single universal equation; it is the process dependence of roughness.

For a helix study, this means β should be interpreted together with f_z. The phase modification introduced by helix acts on the chip-load waveform established by feed per tooth, so changing f_z can alter the observed effect attributed to β.

➢ *Effect of Cutting Speed*

Cutting speed changes the thermal and mechanical state of the cutting zone and also changes the excitation frequency of the machine–tool system. Its influence on roughness can therefore involve wear, deformation, dynamic response, and material behaviour rather than a single monotonic trend.

The relationship can be expressed generically as

$$R\_a = F(V\_c) \qquad (13)$$

Here V_c is cutting speed and F(·) denotes a general process-dependent functional relationship; no specific empirical form is assumed.

Ozcelik and Bayramoglu [2] showed that high-speed end-milling roughness modelling benefits from including process variables and tool operating time. Later prediction studies similarly use heterogeneous measurements, surface-quality descriptors, and simulation-based approaches [30]–[32], supporting the view that roughness response can be nonlinear.

Within the proposed framework, changing V_c also changes spindle speed for a fixed cutter diameter and therefore changes tooth-passing frequency. The same speed change can consequently influence both cutting physics and the relation between excitation and structural modes.

➢ *Effect of Axial and Radial Depth of Cut*

Axial and radial engagement determine how much of the cutting edge is active and therefore influence load magnitude, heat generation, and dynamic behaviour. Optimization studies explicitly include depth of cut among variables affecting force and surface quality [1], [25], [26].

The ideal geometric contribution should be distinguished from these process-induced effects. In the side-milling formulation of Buj-Corral et al. [4], the geometric texture was controlled primarily by feed, tool geometry, eccentricity, and helix. Surface-reconstruction studies [11]–[13], [32] likewise show that additional displacement mechanisms can be superimposed on the ideal kinematic envelope.

Once deflection, vibration, wear, and runout are present, changes in a_p and a_e can modify the measured roughness indirectly by changing the active cutting length and the resulting force and dynamic response.

➢ *Critical Review of Helix-Angle Studies*

Zagórski et al. [18] investigated several cutting-edge helix angles during finish milling of AZ31B and AZ91D magnesium alloys while varying cutting speed, feed per tooth, axial depth, and radial depth. The study is useful here because helix was treated as a controllable geometric factor within a broader process space.

Sur et al. [19] compared fixed- and variable-helix tools in peripheral milling of Ti6Al4V and considered force and roughness together. Their work supports a coupled interpretation in which helix affects both the mechanical load and the resulting surface response.

ISSN No:-2456-2165 https://doi.org/10.38124/ijisrt/26aug534

Hu et al. [20] examined variable-helical milling of titanium alloy TC4 with attention to force, stability, and machining performance. Yang and Liu [17] reported effects of variable pitch on surface plastic deformation and topography. Together with the stability studies [8], [9], [14], [15], these works suggest that helix and pitch variations influence both surface formation and regenerative dynamics.

Taken together, the studies do not justify treating helix as exclusively geometric or exclusively dynamic. Its effect can enter the surface through the ideal cutting envelope and through the load distribution that excites the machine–tool system.

The recent literature strengthens this interpretation. Ding et al. [34] introduced a helix-angle-differentiation approach for modelling forces in gradient-helix end mills, while Sönmez [35] experimentally linked helix, cutting conditions, and tool wear with surface roughness in helical plunge milling of AISI 1045. These papers provide current evidence for coupling geometry with force and surface response.

- *Proposed Theoretical Framework*

Figure 8 summarizes the proposed hierarchy from tool geometry and process settings to chip load, force, dynamic response, surface texture, and roughness.

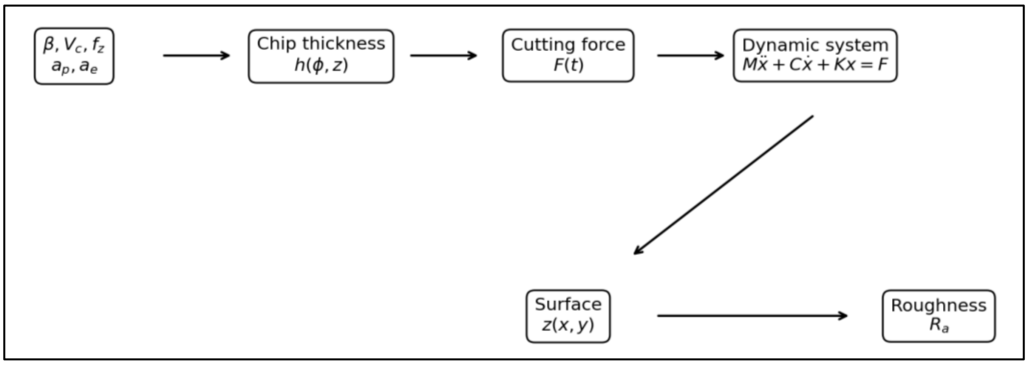

Fig 8 Proposed Theoretical Framework for Helix-Angle-Dependent Surface Roughness.

Figures 6 and 7 provide the intermediate mechanism and surface representation; Fig. 8 condenses these links into a single modelling hierarchy. The formulation below is intended to guide future calibration rather than to assert a universal predictive law.

The central functional representation proposed in this review is

$$R\_a = F(\beta, V\_c, f\_z, a\_p, a\_e, D, z, F\_c, x\_d, W, E) \qquad (14)$$

In Eq. (14), β is helix angle; V_c is cutting speed; f_z is feed per tooth; a_p and a_e are axial and radial depths of cut; D is cutter diameter; z is tooth count; F_c represents cutting-force response; x_d denotes dynamic displacement; W represents tool-wear state; and E represents geometric errors such as runout or eccentricity.

A useful hierarchical form is

$$R\_a = R\_a, g + R\_a, d + R\_a, w + R\_a, e \qquad (15)$$

The terms in Eq. (15) retain the meanings introduced in Eq. (10): geometric, dynamic, wear-related, and geometric-error contributions.

Equation (15) is a conceptual hierarchy. The contributions are not assumed to be independent or strictly additive over all operating conditions; interaction effects are expected and are represented explicitly in Eq. (20).

With

$$R\_a, g = f(f\_z, D, z, a\_e, \beta) \qquad (16)$$

Here R_(a,g) denotes the geometric component of roughness and is written as a function of f_z, D, z, a_e, and β.

$$R\_a, d = f(F\_c, \beta, M, C, K) \qquad (17)$$

In Eq. (17), R_(a,d) denotes the dynamic contribution; F_c is the cutting-force response; β is helix angle; and M, C, and K describe equivalent system mass, damping, and stiffness.

$$R\_a, w = f(V\_c, f\_z, t) \qquad (18)$$

Here R_(a,w) denotes the wear-related contribution; V_c is cutting speed, f_z is feed per tooth, and t denotes machining or tool-operating time.

$$R\_a, e = f(e, \beta) \qquad (19)$$

In Eq. (19), R_(a,e) denotes the geometric-error contribution; e represents eccentricity or runout magnitude and β is helix angle.

Equations (14)–(19) specify the variables and causal links that a future calibrated model should preserve. They do not supply numerical coefficients and should not be interpreted as experimentally validated prediction equations.

A second-order response-surface representation for future experimental validation could be written as

$$R\_a = b\_0 + \Sigma\, b\_i\, X\_i + \Sigma\, b\_ii\, X\_i^2 + \Sigma\, b\_ij\, X\_i\, X\_j \qquad (20)$$

ISSN No:-2456-2165 https://doi.org/10.38124/ijisrt/26aug534

In Eq. (20), b_0 is the intercept; b_i are linear coefficients; b_{ii} are quadratic coefficients; b_{ij} are interaction coefficients; and X_i, X_j are coded experimental factors such as helix angle, cutting speed, feed per tooth, and depth of cut.

With β included among the coded factors, interactions such as $\beta \times f_z$ and $\beta \times V_c$ can test whether the influence attributed to helix changes with process conditions. Their significance and magnitude must be determined experimentally.

III. LITERATURE COMPARISON

For comparison, the literature is arranged into four streams: geometric surface generation; mechanistic force modelling; variable-helix and variable-pitch stability; and empirical/statistical roughness prediction.

The first stream explains how the cutter geometry is mapped onto the workpiece surface [4], [11]–[13], [32]. The second addresses the dependence of cutting forces and coefficients on helix and tool geometry [5]–[7], [21]–[24]. The third concerns regenerative phase and chatter behaviour [8], [9], [14], [15]. The fourth contains studies relating process variables, tool state, and material to measured or predicted roughness [1]–[3], [18]–[20], [25]–[33].

The proposed framework is the connection among these streams: geometry defines the nominal path, force modifies the mechanical state, dynamics modify the actual path, and the resulting texture is quantified by roughness parameters.

➢ *Research Gaps*

Four limitations are particularly evident. First, many studies optimize process settings while holding cutter geometry fixed, whereas fewer treat helix as a primary factor in the same design space as feed, speed, and engagement. Second, helix-angle findings are strongly dependent on material, cutter architecture, and immersion conditions, which makes a universal optimum difficult to transfer. Third, scalar R_a values can conceal directional and three-dimensional texture changes. Fourth, geometry, force, dynamics, wear, and runout are rarely calibrated together in one study.

A useful next step is therefore a controlled design in which helix angle, feed per tooth, cutting speed, axial and radial depth, cutter diameter, tooth count, force, vibration, runout, and wear are recorded in the same experimental campaign. Three-dimensional parameters such as S_a and S_z should complement R_a and R_z.

➢ *Proposed Experimental Validation*

The present manuscript stops at the theoretical level. Equations (14)–(20) specify a structure for a future model, but the coefficients and any material-specific functional forms must be obtained from controlled measurements.

A validation experiment could use several helix-angle levels—for example β = 20°, 35°, and 50°—together with multiple feed-per-tooth and cutting-speed levels. Those levels should be selected from the manufacturer's recommended operating range for the selected tool/workpiece pair; the values are examples, not results of the present study.

Cutting force and vibration should be acquired concurrently with R_a, R_z, S_a, and S_z. Tool runout and wear should be measured independently so that their effects are not absorbed into a single roughness response. This arrangement would permit the proposed geometric, force, dynamic, wear, and error terms to be tested.

ANOVA and response-surface methods can then quantify main effects, curvature, and interactions. A separate confirmation run at the predicted optimum would be needed before any claimed optimum helix angle or predictive equation could be considered experimentally supported.

IV. CONCLUSIONS

This review synthesizes published evidence on how helical cutter geometry and milling conditions can contribute to peripheral-milling surface formation. The conclusions are therefore literature-based interpretations and hypotheses for subsequent testing.

- A larger helix angle produces a larger axial phase difference along a helical cutting edge, providing a direct geometric route to changes in chip-load distribution.
- Feed per tooth sets the nominal chip-load scale and tooth-path spacing; its interaction with helix should therefore be considered when comparing surface-quality results.
- Cutting speed and engagement influence surface response through coupled thermal, mechanical, wear, and dynamic mechanisms, so a universal monotonic roughness trend should not be assumed.
- Helix can influence the finished surface both through the ideal geometric envelope and through force redistribution that changes deflection and vibration.
- Variable-helix and variable-pitch studies indicate that tool geometry can change regenerative phase relationships and hence milling stability.
- The reviewed evidence does not support a transferable optimum helix angle independent of material, cutter geometry, engagement, feed, speed, stiffness, runout, and tool condition.
- The proposed hierarchy provides a testable route from helix geometry and process settings to force, dynamics, surface texture, and roughness; numerical calibration remains a task for future experiments.

The four evidence streams are complementary rather than interchangeable. Mechanistic force studies [21]–[24] explain the load pathway; roughness and optimization studies [25]–[30] quantify process sensitivity; surface-quality and simulation studies [31], [32] describe texture formation; and helix-specific investigations [18]–[20], [33]–[35] provide direct evidence for geometry-dependent behaviour.

ISSN No:-2456-2165 https://doi.org/10.38124/ijisrt/26aug534

Table 1 Selected Literature on Helix Angle, Surface Quality, Force, and Stability

Study	Focus	Variables	Contribution
Buj-Corral et al. [4]	Side milling	feed, eccentricity, helix	Surface-topography model
Wan et al. [5]	Peripheral milling	helix, force	Analytical force mechanism
Ozturk et al. [6]	Force coefficients	helix	Tool-design prediction
Kao et al. [7]	Flat-end milling	helix, geometry	Virtual force model
Sims et al. [8]	Stability	variable pitch/helix	Chatter prediction
Niu et al. [15]	Stability	helix, pitch, runout	Multi-regenerative model
Zagórski et al. [18]	Finish milling	helix, Vc, fz, ap, ae	Experimental roughness study
Sur et al. [19]	Peripheral milling	helix, Vc, feed	Force/roughness optimization
Kowalczyk & Tomczyk [33]	Milling NiTi	helix, coating, feed	Recent force/roughness study
Ding et al. [34]	Force modelling	gradient helix, helix angle	Helix-angle-differentiated force model
Sönmez [35]	Helical plunge milling	helix, cutting conditions, wear	Surface roughness and tool-wear evidence

Notation. Unless otherwise stated, β denotes helix angle, V_c cutting speed, V_f feed velocity, f_z feed per tooth, a_p axial depth of cut, a_e radial depth of cut, D cutter diameter, z number of teeth, and R_a arithmetic average surface roughness. The symbols M, C, and K denote the equivalent dynamic mass, damping, and stiffness of the machining system.

REFERENCES

[1]. J.Z. Zhang, J.C. Chen, E.D. Kirby, Surface roughness optimization in an end-milling operation using the Taguchi design method, J. Mater. Process. Technol. 184 (2007) 233–239. doi:10.1016/j.jmatprotec.2006.11.029.

[2]. B. Ozcelik, M. Bayramoglu, The statistical modeling of surface roughness in high-speed flat end milling, Int. J. Mach. Tools Manuf. 46 (2006) 1395–1402. doi:10.1016/j.ijmachtools.2005.10.005.

[3]. M. Brezocnik, M. Kovacic, M. Ficko, Prediction of surface roughness with genetic programming, J. Mater. Process. Technol. 157–158 (2004) 28–36. doi:10.1016/j.jmatprotec.2004.09.004.

[4]. I. Buj-Corral, J. Vivancos-Calvet, A. Domínguez-Fernández, R. Casado-López, Influence of feed, eccentricity and helix angle on topography obtained in side milling processes, Int. J. Mach. Tools Manuf. 51 (2011) 889–897. doi:10.1016/j.ijmachtools.2011.08.001.

[5]. M. Wan, J. Feng, W.-H. Zhang, Y. Yang, Y.-C. Ma, Working mechanism of helix angle on peak cutting forces together with its design theory for peripheral milling tools, J. Mater. Process. Technol. 249 (2017) 570–580. doi:10.1016/j.jmatprotec.2017.06.030.

[6]. E. Ozturk, O. Ozkirimli, T. Gibbons, M. Saibi, S. Turner, Prediction of effect of helix angle on cutting force coefficients for design of new tools, CIRP Ann. 65 (2016). doi:10.1016/j.cirp.2016.04.042.

[7]. Y.-C. Kao, N.-T. Nguyen, M.-S. Chen, S.-T. Su, A prediction method of cutting force coefficients with helix angle of flat-end cutter and its application in a virtual three-axis milling simulation system, Int. J. Adv. Manuf. Technol. 77 (2015) 1793–1809. doi:10.1007/s00170-014-6550-8.

[8]. N.D. Sims, B. Mann, S. Huyanan, Analytical prediction of chatter stability for variable pitch and variable helix milling tools, J. Sound Vib. 317 (2008) 664–686. doi:10.1016/j.jsv.2008.03.045.

[9]. G. Jin, Q. Zhang, H. Qi, B. Yan, A frequency-domain solution for efficient stability prediction of variable helix cutters milling, Proc. Inst. Mech. Eng. C 228 (2014) 2702–2710. doi:10.1177/0954406214522614.

[10]. E. Ozturk, L.T. Tunc, E. Budak, Investigation of lead and tilt angle effects in 5-axis ball-end milling processes, Int. J. Mach. Tools Manuf. 49 (2009) 1053–1062. doi:10.1016/j.ijmachtools.2009.07.013.

[11]. M. Arizmendi, J. Fernández, A. Gil, F. Veiga, Model for the prediction of heterogeneity bands in the topography of surfaces machined by peripheral milling considering tool runout, Int. J. Mach. Tools Manuf. 50 (2010) 51–64. doi:10.1016/j.ijmachtools.2009.09.007.

[12]. J.-P. Costes, V. Moreau, Surface roughness prediction in milling based on tool displacements, J. Manuf. Process. 13 (2011) 133–140. doi:10.1016/j.jmapro.2011.02.003.

[13]. B. Denkena, M. Krüger, D. Bachrathy, G. Stépán, Model based reconstruction of milled surface topography from measured cutting forces, Int. J. Mach. Tools Manuf. 54–55 (2012) 25–33. doi:10.1016/j.ijmachtools.2011.12.007.

[14]. A.R. Yusoff, N.D. Sims, Optimisation of variable helix tool geometry for regenerative chatter mitigation, Int. J. Mach. Tools Manuf. 51 (2011) 133–141. doi:10.1016/j.ijmachtools.2010.10.004.

[15]. J. Niu, Y. Ding, L. Zhu, H. Ding, Mechanics and multi-regenerative stability of variable pitch and variable helix milling tools considering runout, Int. J. Mach. Tools Manuf. 123 (2017) 129–145. doi:10.1016/j.ijmachtools.2017.08.006.

[16]. E. Diez Cifuentes, H. Pérez García, M. Guzmán Villaseñor, A. Vizán Idoipe, Dynamic analysis of runout correction in milling, Int. J. Mach. Tools Manuf. 50 (2010) 709–717. doi:10.1016/j.ijmachtools.2010.04.010.

[17]. D. Yang, Z. Liu, Surface plastic deformation and surface topography prediction in peripheral milling with variable pitch end mill, Int. J. Mach. Tools

Manuf. 91 (2015) 43–53. doi:10.1016/j.ijmachtools.2014.11.009.
[18]. I. Zagórski, A. Szczepaniak, M. Kulisz, J. Korpysa, Influence of the tool cutting edge helix angle on the surface roughness after finish milling of magnesium alloys, Materials 15 (2022) 3184. doi:10.3390/ma15093184.
[19]. G. Sur, A.R. Motorcu, S. Nohutçu, Single and multi-objective optimization for cutting force and surface roughness in peripheral milling of Ti6Al4V using fixed and variable helix angle tools, J. Manuf. Process. 80 (2022) 529–545. doi:10.1016/j.jmapro.2022.06.016.
[20]. X. Hu, H. Qiao, M. Yang, Y. Zhang, Research on milling characteristics of titanium alloy TC4 with variable helical end milling cutter, Machines 10 (2022) 537. doi:10.3390/machines10070537.
[21]. P. Lee, Y. Altintas, Prediction of ball-end milling forces from orthogonal cutting data, Int. J. Mach. Tools Manuf. 36 (1996) 1059–1072. doi:10.1016/0890-6955(95)00081-X.
[22]. E. Budak, Y. Altintas, E.J.A. Armarego, Prediction of milling force coefficients from orthogonal cutting data, J. Manuf. Sci. Eng. 118 (1996) 216–224. doi:10.1115/1.2831014.
[23]. E.J.A. Armarego, N.P. Deshpande, Force prediction models and CAD/CAM software for helical tooth milling processes. I. Basic approach and cutting analyses, Int. J. Prod. Res. 31 (1993) 1991–2009. doi:10.1080/00207549308956836.
[24]. A. Lamikiz, L.N. Lopez de Lacalle, J.A. Sanchez, U. Bravo, Calculation of the specific cutting coefficients and geometrical aspects in sculptured surface machining, Mach. Sci. Technol. 9 (2005) 411–436. doi:10.1080/15321790500226614.
[25]. N. Masmiati, A.A.D. Sarhan, M.A.N. Hassan, M. Hamdi, Optimization of cutting conditions for minimum residual stress, cutting force and surface roughness in end milling of S50C medium carbon steel, Measurement 86 (2016) 253–265. doi:10.1016/j.measurement.2016.02.049.
[26]. N. Tamiloli, J. Venkatesan, V. Ramnath, A grey-fuzzy modeling for evaluating surface roughness and material removal rate of coated end milling insert, Measurement 84 (2016) 68–82. doi:10.1016/j.measurement.2016.02.008.
[27]. A.B. Sharkawy, Prediction of surface roughness in end milling process using intelligent systems: a comparative study, Appl. Comput. Intell. Soft Comput. 2011 (2011) 183764. doi:10.1155/2011/183764.
[28]. S. Palani, U. Natarajan, Prediction of surface roughness in CNC end milling by machine vision system using artificial neural network based on 2D Fourier transform, Int. J. Adv. Manuf. Technol. 54 (2011) 1033–1042. doi:10.1007/s00170-010-3018-3.
[29]. G. Beruvides, F. Castaño, R.E. Haber, Coping with complexity when predicting surface roughness in milling processes: hybrid incremental model with optimal parametrization, Complexity 2017 (2017) 7317254. doi:10.1155/2017/7317254.
[30]. W.-C. Liu, P. Wang, Y. You, Surface roughness prediction using multi-source heterogeneous data and Bayesian quantile regression in milling process, J. Manuf. Process. 95 (2023) 446–460. doi:10.1016/j.jmapro.2023.04.038.
[31]. X. Wu, Z. Chen, W. Ke, F. Jiang, M. Zhao, J. Shen, L. Zhu, Investigation on surface quality in micro milling of additive manufactured Ti6Al4V titanium alloy, J. Manuf. Process. 101 (2023) 446–457. doi:10.1016/j.jmapro.2023.05.110.
[32]. B. Denkena, M.-A. Dittrich, J. Huuk, Simulation-based surface roughness modelling in end milling, Procedia CIRP 99 (2021) 151–156. doi:10.1016/j.procir.2021.03.096.
[33]. M. Kowalczyk, K. Tomczyk, Quality of machined surface and cutting force when milling NiTi alloys, Materials 17 (2024) 6122. doi:10.3390/ma17246122.
[34]. M. Ding, C. Yue, R. Zhen, X. Liu, S. Sun, S.Y. Liang, L. Wang, Cutting force modeling of the gradient helix edge end mill based on helix angle differentiation, Thin-Walled Structures 215 (2025) 113537. doi:10.1016/j.tws.2025.113537.
[35]. F. Sönmez, Investigation of surface roughness and tool wear in helical plunge milling of AISI 1045 material, Gazi University Journal of Science 38 (2025) 2107–2116. doi:10.35378/gujs.1597747.